

A novel method for determining and improving the quality of a quadrupolar fiber gyro coil under temperature variations

Zhihong Li,^{1,2} Zhuo Meng,^{1,2} Tiegen Liu,¹ and X. Steve Yao^{1,*}

¹Polarization Research Center, College of Precision Instrument & Opto-electronics Engineering and Key Laboratory of Opto-electronics Information and Technical Science, Ministry of Education, Tianjin University, Tianjin 300072, China

²Suzhou Opto-ring Co. Ltd., Suzhou 215123, China

*steveyao888@yahoo.com

Abstract: We introduce a parameter called pointing error thermal sensitivity (PETS) for quantitatively determining the quality of a quadrupolar (QAD) fiber coil under radial temperature variations. We show both analytically and experimentally that the pointing error of a fiber gyro incorporating the fiber coil is linearly proportional to the final radial thermal gradient on the coil, with PETS as the proportional constant. We further show that PETS is linearly proportional to another parameter called effective asymmetric length of the coil. By thermally inducing different radial thermal gradients on the fiber coil and measuring the corresponding pointing errors in a gyroscopic measurement setup, we can confidently determine the PETS of the fiber coil and its associated effective asymmetric length caused by imperfections in coil winding. Consequently, we are able to precisely trim the coil to achieve best thermal performance.

©2013 Optical Society of America

OCIS codes: (060.0060) Fiber optics and optical communications; (060.2430) Fibers, single-mode; (060.2800) Gyroscopes.

References and links

1. V. Vali and R. W. Shorthill, "Fiber ring interferometer," *Appl. Opt.* **15**(5), 1099–1100 (1976).
2. H. C. Lefevre, "Fundamental of interferometric fiber optic gyroscope," in *Fiber Optic Gyros: 20 Anniversary Conf.*, Proc. SPIE **2837**, 46–60 (1996).
3. G. A. Sanders, B. Szafraniec, R. Y. Liu, M. S. Bielas, and L. Strandjord, "Fiber-optic gyro development for a broad range of applications," Proc. SPIE, *Fiber Optic and Laser Sensors XIII* **2510**, 2–11 (1995).
4. G. A. Sanders, B. Szafraniec, R. Y. Liu, C. L. Laskoskie, L. K. Strandjord, and G. Weed, "Fiber optic gyros for space, marine, and aviation applications," in *Fiber Optic Gyros: 20 Anniversary Conf.*, Proc. SPIE **2837**, 61–71 (1996).
5. M. Chomát, "Efficient suppression of thermally induced nonreciprocity in fiber-optic Sagnac interferometers with novel double-layer winding," *Appl. Opt.* **32**(13), 2289–2291 (1993).
6. R. Dyott, "Reduction of the Shupe effect in fibre optic gyros; the random-wound coil," *Electron. Lett.* **32**(23), 2177–2178 (1996).
7. R. P. Goettsche and R. A. Bergh, "Trimming of fiber optic winding and method of achieving same," U.S. Patent: 5528715, 6–18 (1996).
8. F. Mohr, "Thermooptically induced bias drift in fiber optical Sagnac interferometers," *J. Lightwave Technol.* **14**(1), 27–41 (1996).
9. D. M. Shupe, "Thermally induced nonreciprocity in the fiber-optic interferometer," *Appl. Opt.* **19**(5), 654–655 (1980).
10. W. Feng, X. Wang, and W. Wang, "Effect of turns' difference in each layer on temperature performance of fiber optic gyroscope," *Journal of Chinese Inertial Technology* **19**, 487–493 (2011).
11. C. Mao, Z. Gong, X. Mou, and G. Yang, "Finite difference method for temperature field in fiber optical gyroscope," *Piezoelectrics and Acoustooptics* **25**, 98–101 (2003).
12. M. Li, T. Liu, Y. Zhou, J. Jiang, L. Hou, J. Wang, and X. S. Yao, "A 3-D model for analyzing thermal transient effects in fiber gyro coils," Proc. SPIE, *Advanced Sensor Systems and Applications III*, 6830–6834 (2007).
13. C. M. Lofts, P. B. Ruffin, M. D. Parker, and C. C. Sung, "Investigation of the effects of temporal thermal gradients in fiber optic gyroscope sensing coils," *Opt. Eng.* **34**(10), 2856–2863 (1995).
14. J. Sawyer, P. B. Ruffin, and C. Sung, "Investigation of the effects of temporal thermal gradients in fiber optic gyroscope sensing coils, part II," *Opt. Eng.* **36**(1), 29–34 (1997).

1. Introduction

It has been more than 35 years since fiber-optic gyroscope (FOG) was first proposed by V. Vali and R. Shorthill [1]. Nowadays, FOGs are in mass production and are widely used in various military and civilian applications [2–4], such as in aircrafts, vessels, and land vehicles for precision rotation rate and angle detection. A key component in a FOG is a fiber coil, which must be wound painstakingly with special geometries [5–8], such as quadrupolar winding pattern, to reduce a nonreciprocal effect caused by thermal variations known as Shupe effect [9]. Despite a large amount of FOGs have been produced for various applications, the making of good fiber coils still remains a work of art, with large variations in performance for coils made with even the same process. Test standards are available for testing the performance of a whole fiber gyro in operation, including combined contributions from the light source, Y-coupler, passive components, fiber coil, mechanical structure and enclosure, and electronics. However, to the best of authors' knowledge, no published test standards or comprehensive methods are available for testing a fiber coil's performance under temperature variations alone, although some attempts were made to measure coils asymmetry with inconclusive results [10]. Such a test is important for ensuring that good quality fiber coils can be mass produced with good uniformity and efficiency. In order to determine the quality of a coil alone, meaningful test parameters and associated test methods must be defined and developed. Such a parameter can relate to winding imperfections for engineers to find out the root causes of the problem coils, and implement corrective measures or process improvements.

In this paper, we introduce a parameter called pointing error thermal sensitivity (PETS) for quantifying the performance of a quadrupolar fiber coil subject to a time-dependent radial temperature gradient. We show that the pointing error (asymptotic angular error) of a gyro system incorporating the quadrupolar fiber coil is linearly proportional to the final temperature gradient between the inner and outer coil surfaces in the radial direction, with PETS as the proportional constant. We further show that PETS is linearly proportional to a parameter called effective asymmetric length of the fiber coil, caused by imperfections in fiber winding. In addition, by thermally inducing different time-varying radial temperature gradients on the fiber coil (as will be shown in inset b of Fig. 3) and measuring the corresponding pointing errors in a gyroscopic measurement setup, we can confidently determine the PETS of the fiber coil and its associated effective asymmetric length. Such parameters can be directly used to trim the fiber coil [7, 11] for better temperature performance, feedback to coil production for improving winding process, or simply be used to quantitatively determine the quality of fiber gyro coils. Finally, we trim multiple coils according to the obtained asymmetric lengths to achieve best thermal performance, and experimentally verify the usefulness and correctness of the PETS definition and the asymmetry length relations.

It should point out that our experiments indicate that the PETS measurement results are robust against environment temperature variations and sensitive only to coil's asymmetry, and therefore is a practical parameter for characterizing the thermal performance of fiber coils, determining the coil asymmetry length, and guiding the coil trimming.

2. Pointing error caused by time-dependent radial thermal gradient

In this section, we first derive an expression for the angular error of a gyro system incorporating an imperfectly wound fiber coil with a certain length asymmetry. We then introduce and define PETS to describe the performance of the coil against temperature variations, and another parameter called effective asymmetric length to reflect the accumulative winding imperfections.

With the origin of the coordinate located at the fiber coil midpoint $s = L/2$ (L is the total fiber length), the nonreciprocal phase shift $\Delta\varphi_e$ induced by the Shupe effect in the single-mode fiber can be expressed as [12–14]:

$$\Delta\varphi_e(t) = \frac{2\tau}{L} \beta_0 \frac{\partial n}{\partial T} \left[\int_0^{L/2} \frac{\partial T(s,t)}{\partial t} s ds - \int_0^{L/2} \frac{\partial T(s',t)}{\partial t} s' ds' \right] \quad (1)$$

where τ is the transit time of light through the fiber coil, $\beta_0 = 2\pi/\lambda_0$ is the wave number, n is the effective refractive index, $\partial n/\partial T$ is its temperature coefficient, $\partial T(s,t)/\partial t$ is the temperature variation along the fiber, and s and s' are distances along the fiber coil. They are both positive, but are measured in opposite directions, with s increasing in the clockwise (CW) direction and s' in the counter clockwise (CCW) direction.

Accordingly, the rotation rate error induced by a thermal transient is:

$$\Omega_e(t) = \frac{4\gamma}{L} \left[\int_0^{L/2} \frac{\partial T(s,t)}{\partial t} s ds - \int_0^{L/2} \frac{\partial T(s',t)}{\partial t} s' ds' \right] \quad (2)$$

where γ is a parameter relating to the thermal coefficient of the fiber and the diameter D of the coil and is defined as:

$$\gamma = \frac{n}{2D} \frac{\partial n}{\partial T} \quad (3)$$

By integrating the rate error $\Omega_e(t)$ over time, the pointing error (asymptotic angular error) ψ_e induced by the temperature variation is obtained as:

$$\psi_e(t') = \int_0^{t'} \Omega_e(t) dt = \frac{4\gamma}{L} \left[\int_0^{L/2} \Delta T(s,t') s ds - \int_0^{L/2} \Delta T(s',t') s' ds' \right] \quad (4)$$

where $\Delta T(s,t) = T(s,t) - T(s,0)$.

For a quadrupole-wound coil with 8 layers of fiber shown in Fig. 1(a), we use full lines labeled A to denote fiber layers winding in the CCW direction and broken lines labeled B to denote the fiber layers winding in the CW direction [7]. As shown in Fig. 1(b), we use A_i and B_i to number the fiber layers in CCW and CW directions respectively. The corresponding quadrupolar winding pattern can therefore be described as ABBA-ABBA. In Table 1, we designate fiber layer numbers and list the height and length of each fiber layer.

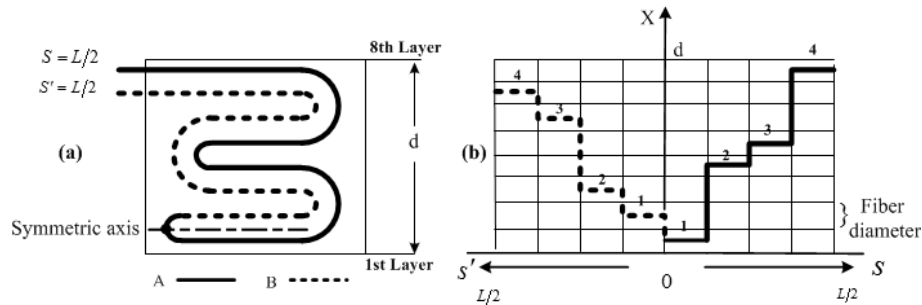


Fig. 1. Illustration of a quadrupole-wound fiber coil, where A and B are used to denote fiber layers wound in CCW (solid line) and CW (broken line) directions respectively, and d is the fiber coil thickness. (a) The relative positions of CCW and CW layers. (b) The numbering of each fiber layer in CCW and CW directions, where the height of each grid cell indicates the diameter of the fiber and the lines represent the position of fiber's center line in the vertical axis.

We examine the case in which the temperature variation is only along the radial direction of the coil, and is independent of the axial position and azimuth angle. Therefore, the temperature on each fiber layer is constant and Eq. (4) can be simplified to the following

expression, assuming that the fiber coil is symmetrically wound around coil midpoint, as illustrated in Fig. 2(a):

$$\psi_{e0}(t) = \frac{4\gamma}{L} \sum_{i=1}^4 [\Delta T(A_i, t) - \Delta T(B_i, t)] \cdot \int_{(i-1)L/8}^{iL/8} s \cdot ds \quad (5)$$

Table 1. Height and Length of Each Fiber Layer

Winging pattern	A	B	B	A	A	B	B	A
Global layer number	1	2	3	4	5	6	7	8
CCW layer number	1			2	3			4
CCW layer length (m)	0~L/8			L/8~L/4	L/4~3L/8			3L/8~L/2
CCW layer height (m)	d/16			7d/16	9d/16			15d/16
CW layer number		1	2			3	4	
CW layer length (m)		0~L/8	L/8~L/4			L/4~3L/8	3L/8~L/2	
CW layer height (m)		3d/16	5d/16			11d/16	13d/16	

However, if the coil is not wound perfectly symmetric, the position of the midpoint where two counter propagating light waves meet will change. As shown in Fig. 2(b), if the CCW wound fiber (denoted by A) is shortened by l , the midpoint for the counter-propagating light waves to meet will move to the longer fiber side (denoted by B) by $l/2$. In practice, even if the fiber lengths for CCW and CW fiber sections are the same, the optical path lengths may be different due to refractive index variations along the fiber caused by imperfection of the fiber and different stresses on the fiber. Therefore, we introduce a quantity called effective asymmetric length l_{eff} to denote the shortened optical path length of CCW fiber section, which will result in a shift of coil midpoint by $l_{eff}/2$ fiber length to the CW section. Consequently, the pointing error resulting from such an imperfect coil can be expressed as:

$$\psi_e(t) = \frac{4\gamma}{L} \left\{ \sum_{i=1}^4 [\Delta T(A_i, t) - \Delta T(B_i, t)] \cdot \int_{(i-1)\frac{L-l_{eff}}{8}}^{\frac{L-l_{eff}}{8}} s \cdot ds + \sum_{i=1}^3 [\Delta T(A_i, t) - \Delta T(B_{i+1}, t)] \cdot \int_{\frac{L-l_{eff}}{8}}^{\frac{L-l_{eff}}{8} + \frac{l_{eff}}{2}} s \cdot ds \right\} \quad (6)$$

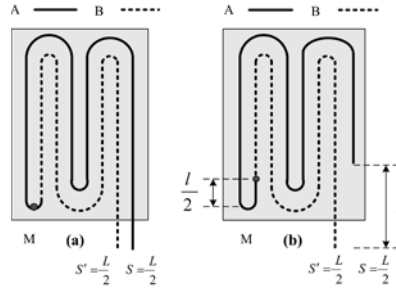


Fig. 2. Illustration of asymmetrical fiber winding. (a) CCW (denoted by A) and CW (denoted by B) wound fiber sections have the same length. (b) CWW section is short by a length of l , resulting in a shift of $l/2$ of the coil midpoint to the CW side.

The total accumulated angular error ψ_e (pointing error), which reflects the performance of the fiber coil under a temperature variation, can be determined at thermal equilibrium ($t \rightarrow \infty$) when the thermally induced nonreciprocity in the fiber coil diminishes. Note that the temperature change $\Delta T(x)$ on each layer can be described as follows:

$$\Delta T (A_i) = \Delta T_{inner} + \delta T \frac{x_i}{d}, (x_i = d/16, 7d/16, 9d/16, 15d/16) \quad (7a)$$

$$\Delta T (B_i) = \Delta T_{inner} + \delta T \frac{x_i}{d}, (x_i = 3d/16, 5d/16, 11d/16, 13d/16) \quad (7b)$$

where $\delta T = \Delta T_{outer} - \Delta T_{inner}$, $\Delta T_{outer} = TC_1 - T_{room}$, $\Delta T_{inner} = TC_2 - T_{room}$, T_{room} is the room temperature, and d is the coil width.

Substitution of (7) in (5) and (6) yields:

$$\psi_{e0} = \gamma \frac{L}{8^2} \delta T \quad (8a)$$

$$\psi_e = \gamma \left(\frac{L}{8^2} - \frac{7}{8} l_{eff} \right) \delta T \quad (8b)$$

where ψ_{e0} and ψ_e are the pointing errors for coils without and with winding induced length asymmetry l_{eff} .

It can be shown that for a fiber coil with N layers, the pointing errors caused by a radial temperature variation can be expressed as:

$$\psi_{e0} = \gamma \frac{L}{N^2} \delta T \quad (9a)$$

$$\psi_e = \gamma_T \delta T = \psi_{e0} - \frac{N-1}{N} (\gamma \delta T) l_{eff} \quad (9b)$$

$$\gamma_T = \gamma \left(\frac{L}{N^2} - \frac{N-1}{N} l_{eff} \right) = \gamma \cdot l_{all} \quad (9c)$$

where $l_{all} = L/N^2 - (N-1)/N \cdot l_{eff}$ is the overall asymmetric length of the coil to be discussed shortly.

γ_T is an important parameter and is named as the pointing error thermal sensitivity (PETS) of the coil. It is directly proportional to coil's asymmetric length, and as will be shown next, it can be obtained experimentally by changing δT while measuring the pointing error ψ_e .

Although a similar equation to Eq. (9a) for a perfect symmetric quadruple-winding coil was obtained previously [8], it cannot be used to evaluate imperfect fiber coils. As will be shown next, Eq. (9b) obtained in this paper is the most important equation for characterizing the symmetry property of a quadruple-winding fiber coil.

It is interesting to notice from Eq. (9c) that for a perfect geometrically symmetric coil ($l_{eff} = 0$), the thermally induced pointing error is non-zero and decreases quadratically with N . The pointing error can be reduced to zero if an asymmetry $l_{eff} = L/[N(N-1)]$ is purposely introduced. Such an asymmetry is understandable, considering that the "A" portion fiber has two layers at the inner and outer most surfaces, as shown in Fig. 1 and Fig. 5(a), and they are impacted more by the temperature changes than the "B" layers beneath them. Consequently "A" portion should be shortened to match the temperature effect on the "B" portion by $L/[N(N-1)]$. In other words, $L/[N(N-1)]$ is the intrinsic asymmetric length relating to quadruplar winding pattern and can be compensated by trimming "A" portion fiber by the equal amount. For a fiber coil with 8 and 24 layers, the required trimming lengths

are 1.78% and 0.18% of the coil length, respectively. Therefore, we introduced an overall coil asymmetric length l_{all} in Eq. (9c) to take into account of both intrinsic and winding asymmetries.

3. Experimental result and discussions

Three frameless SM fiber coils with conductive potting adhesives are used in this study and all of them were wound with the quadrupolar winding scheme. The coils are approximately 1.25cm in height with an inner diameter of 5.3cm. The total length of fiber on each coil is 240m, producing 24 fiber layers. Each fiber coil is placed in an open-loop gyroscopic setup shown in Fig. 3 to form a complete fiber gyro and to be evaluated for its thermal performance. As shown in insets a) and b), a temperature gradient is applied to a coil in the radial direction such that the fiber in each layer experiences the same temperature. The temperatures both at coil's inner and outer surfaces were monitored with two separate thermocouples. In the experiments, we always keep the lengths of fiber pigtailed constant at 2 meters each.

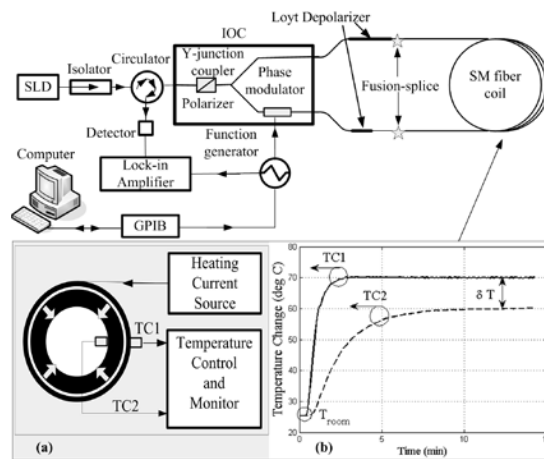


Fig. 3. Gyroscopic setup for measuring thermal induced error signals. Inset a) shows a ribbon heater with a width and a length equal to the width and the perimeter of the coil is wrapped around coil to apply a radial temperature gradient. TC1 and TC2 are the temperatures measured at the outer and inner surfaces of the fiber coil. Inset b) shows TC1 and TC2 as a function of time when a radial temperature excitation is applied, and are stabilized at 70.2°C and 54.3°C respectively, resulting a temperature gradient $\delta T = TC1 - TC2 = 15.9$ °C

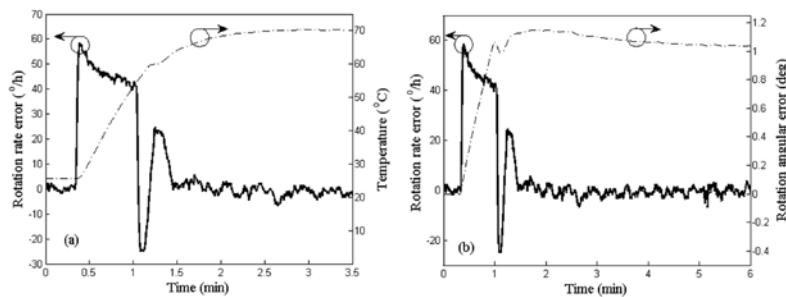


Fig. 4. (a) Measured rotation rate error (solid line) of a gyro system in Fig. 3 when the fiber coil's outer layer is subject to a temperature change TC1 (dotted line). (b) Angular error of the gyro system steadily approaches asymptotic value (pointing error), despite the fast fluctuation of the corresponding rate error (solid line).

A varying temperature gradient on the fiber coil will cause a nonreciprocal phase shift, which will result in rotation rate and pointing errors for a gyro system incorporating the fiber coil. Figure 4(a) shows the rotation rate error of a gyro system in Fig. 3 as a function of time when a temperature gradient shown in the insets of Fig. 3 is applied to the fiber coil. By integrating the rate error $\Omega_e(t)$ over time, the angular error can be obtained, as shown in Fig. 4(b). It should be pointed out that the angular error signal steadily approaches an asymptotic value ψ_e around 1.04 degrees (pointing error), despite large fluctuations of the measured rate error.

3.1 Experimental verification of Eq. (9)

Equation (9b) shows that the pointing error is linearly proportional to the effective asymmetry length l_{eff} of the coil and can be experimentally verified by fixing δT while changing l_{eff} by trimming the length of “A” side (e.g. CCW side) of the coil. In Eq. (9b), the effective asymmetry length l_{eff} can be expressed as:

$$l_{eff} = l_{eff0} + l \quad (10a)$$

where l_{eff0} is the initial effective asymmetry length before trimming the coil and l is the trimming length. Substitution of Eq. (10a) in Eq. (9b) yields:

$$\psi_e = \psi'_{e0} - \frac{N-1}{N}(\gamma\delta T) \cdot l \quad (10b)$$

where the pointing error before coil trimming ($l = 0$) is

$$\psi'_{e0} = \psi_{e0} - \frac{N-1}{N}(\gamma\delta T) \cdot l_{eff0} \quad (10c)$$

When trimming a coil, we unwrap some turns from the coil outer layer (“A” side or CCW side), as shown in Fig. 5(a) and cut a length of fiber equal to the unwrapped portion to keep the fiber pigtail length constant. The trimming length l is defined positive when cutting fiber from the outer layer (“A” side) of a coil.

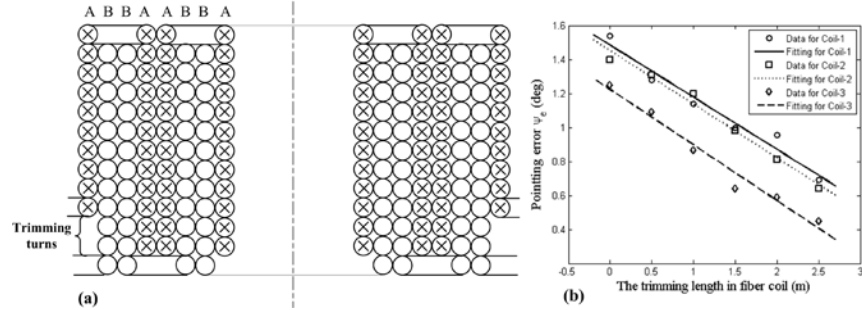


Fig. 5. (a) Illustration of coil trimming with two fiber turns unwrapped from the outer layer of the coil. (b) Measured pointing error ψ_e of fiber coil as a function of the trimming lengths l when a temperature excitation profile from room temperature to 70°C is applied to the outer layer of the coil.

We trimmed and tested three fiber coils of the same diameter and made with the same fiber. The measured pointing error ψ_e of the gyro system incorporating the coils as the function of the trimming length l is shown in Fig. 5(b). The same temperature profile shown in Fig. 3 was applied to each coil’s outer layer and each coil is trimmed at six trimming lengths ($l = 0\text{m}, 0.5\text{m}, 1\text{m}, 1.5\text{m}, 2\text{m}, 2.5\text{m}$). It is evident that the pointing error is linearly

proportional to the trimming lengths l and hence to the effective asymmetry length l_{eff} , agrees well with Eq. (9b). Because the three coils have the same diameters and are made with the same fibers, γ in Eq. (9) are expected to be the same according to Eq. (3). In addition, the temperature gradients applied to the three coils are also the same so that the slope $(N-1)/N \cdot \gamma \delta T$ in Eq. (9b) of the three coils are also expected to be the same. Indeed, the experimental results in Fig. 5(b) agree well with the prediction of Eq. (9b). It is important to point out that by curve fitting to Eq. (9b) one can obtain $\gamma \delta T$ and consequently γ because δT can be obtained independently in the experiment.

Table 2. Measurement Results of $\gamma \delta T$ and ψ'_{e0} of Three Fiber Coils

	Coil-1	Coil-2	Coil-3
Measured δT	15.86	15.43	15.3
$(N-1)/N \cdot \gamma \delta T$	0.311	0.315	0.321
γ	0.0188	0.0196	0.0201
ψ'_{e0} (Deg)	1.483	1.451	1.223

Table 2. shows the slope $\gamma \delta T$ and the intercept ψ'_{e0} of each fiber coil. The slopes are slightly different due to the slightly fluctuation of δT among three coils, possibly caused by non-identical winding and potting of the coils. The average γ obtained for this coil type is $0.0195 / (^{\circ}\text{C} \cdot \text{m})$ (for each coil type γ can be determined by performing the trimming procedure described above). The different intercepts ψ'_{e0} of the three curves in Fig. 5(b) and in Table 2 indicate that the three coils have different initial effective asymmetric lengths l_{eff0} , according to Eq. (10c).

3.2 Determination of coil's pointing error thermal sensitivity and asymmetric length

After verifying Eq. (9) experimentally, we now can confidently use it to determine the pointing error thermal sensitivity (PETS) γ_T of a fiber coil and its effective asymmetric length l_{eff} by measuring ψ_e at different δT .

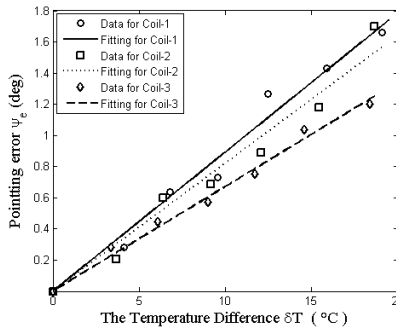


Fig. 6. The pointing error taken before coil trimming. The lines indicate the best linear fit through the data points.

Using the setup in Fig. 3, we applied six different temperature excitation profiles to the outer layer of each coil ($TC_2 = 30^{\circ}\text{C}, 40^{\circ}\text{C}, 50^{\circ}\text{C}, 60^{\circ}\text{C}, 70^{\circ}\text{C}, 80^{\circ}\text{C}$). The corresponding temperature differences δT for the three coils are shown in Table 3. Figure 6 shows the measured ψ_e as a function of δT of the three coils without trimming. The pointing error

increases linearly with δT , agreeing well with Eq. (9b). By curve-fitting ψ_e to Eq. (9b), we obtain PETS γ_T of three coils and the results are shown in Table 3.

Table 3. Outer Surface Temperature, Final Temperature Gradient, and γ_T of Three Coils Under Test

Outer surface temperature (°C)		30	40	50	60	70	80	γ_T (deg / °C)
δT (°C)	Coil-1	4.11	6.80	9.55	12.49	15.86	19.06	0.086
	Coil-2	3.68	6.40	9.15	12.09	15.43	18.65	0.083
	Coil-3	3.37	6.11	8.99	11.72	15.3	18.38	0.067

From Eq. (9c), we obtain the overall asymmetry lengths l_{all} of the three coils as 4.3 m, 4.1 m, and 3.33 m respectively, where $\gamma = 0.0195$ is used in the calculation. The corresponding effective asymmetric lengths $l_{eff 0}$ of the coils from winding imperfections can be found as:

$$l_{eff 0} = L/[N(N-1)] - N \cdot l_{all}/(N-1) \quad (11)$$

Substitution of $L = 240\text{m}$ and $N = 24$ in Eq. (11), we obtain the initial effective asymmetry lengths of the three coils as -4.16m , -3.98m and -3.12m , respectively. The minors sign indicates that the length of “A” portion fiber is longer than that of “B” portion fiber in the coils.

We further measured the pointing error as a function of final temperature gradient of the three coils with different trimming lengths, with the result of coil-2 shown in Fig. 7(a). Clearly, pointing error is almost insensitive to variations in thermal gradient with a trimming length about 4.5 m, corresponding to a near zero overall asymmetric length. Pointing error starts to increase in the negative direction with the thermal gradient when the coil is over trimmed with a trimming length of 5 m. These results are consistent with the prediction of Eqs. (9b) and (9c). Evidently, PETS is an excellent parameter to quantify the thermal performance of fiber coils: a larger PETS corresponds to a larger overall asymmetric length. The smaller the PETS of a coil, the smaller the thermal induced pointing error of the gyro incorporating the coil.

Figure 7(b) shows PETS obtained by curve fitting in Fig. 7(a) as a function of trimming length. The solid line is the plot of Eq. (9c) using experimental parameters ($L = 240\text{m}$, $N = 24$ and $\gamma = 0.0195 / (^\circ\text{C} \cdot \text{m})$), and it agrees with the experimental data reasonably well.

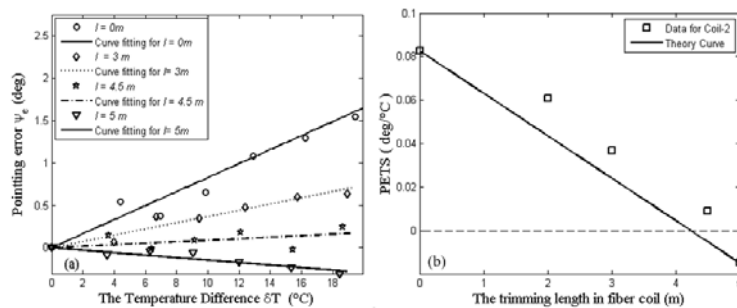


Fig. 7. (a) Pointing error of Coil-2 with different trimming lengths on the “A” portion fiber. The slope of each curve is the PETS of the coil. (b) PETS of Coil-2 as a function of trimming length l and the corresponding theoretical curve of Eq. (9c) for $L = 240\text{m}$, $N = 24$ and $\gamma = 0.0195$

4. Summary

In summary, we have proposed and demonstrated a practical approach to quantitatively determine the performance of a fiber gyro coil subject to thermal variations. We show both theoretically and experimentally that the pointing error of a fiber gyro is linearly proportional to its fiber coil's radial thermal gradient, and define the proportional constant as the pointing error thermal sensitivity (PETS) to quantify the thermal performance of fiber coils. In addition, we introduce a parameter called overall asymmetric length of the coil and show that it includes two contributions: one is intrinsic to the coil winding pattern and the other from imperfections made during coil winding. We further show both analytically and experimentally that the asymmetric length is linearly proportional to PETS and can be obtained once PETS is measured by measuring the pointing error as a function of radial thermal gradient. Finally, we prove experimentally that the thermal sensitivity of a fiber coil can be reduced to near zero by trimming the fiber coil by the amount equaling the overall asymmetric length obtained.

Our experiments indicate that the proposed PETS measurement is robust against environment temperature variations and sensitive only to coil's asymmetry, and therefore is a practical parameter for determining the thermal performance of fiber coils, determining the coil asymmetry length, and guiding the coil trimming. More experiments are under the way to quantitatively determine the influence, if any, of environmental temperature on PETS measurements.

Acknowledgments

This work was supported by the National Basic Research Program of China (973 Program) under grant 2010CB327806, International Science & Technology Cooperation Program of China under Grants No. 2009DFB10080 and No. 2010DFB13180, China Postdoctoral Science Foundation under Grant No. 20100470782.